Conclusions

The analytical techniques used during the test program permitted accurate pretest predictions. These techniques are being applied in the NERVA flight-engine program and will greatly reduce the number of tests required at the subsystem and engine level. This proven analytical approach grants a higher confidence of success with a limited number of tests.

References

[1] Rice, C. M. and Arnold, W. H., "Recent NERVA Technology Development," *Journal of Spacecraft and Rockets*, Vol. 6, No. 5, May 1969, pp. 565–569.

[2] Buden, D., "Operational Characteristics of Nuclear Rockets," *Journal of Spacecraft and Rockets*, Vol. 7, No. 7, July 1970, pp. 832–836.

DECEMBER 1970 J. SPACECRAFT VOL. 7, NO. 12

Analysis of Solid Teflon Pulsed Plasma Thruster

ROBERT J. VONDRA*
Lincoln Laboratory, Massachusetts Institute of Technology, Lexington, Mass.

AND

KEITH THOMASSEN† AND ALBERT SOLBES‡
Massachusetts Institute of Technology, Cambridge, Mass.

Studies of the pulsed plasma thruster used for stationkeeping in the LES-6 satellite are described. Current waveforms were measured, from which circuit parameters were deduced, an energy balance made, and thrust was computed. Each current pulse ablates $\sim 10^{-8}$ kg of Teflon (6×10^{16} molecules of C_2F_4), exhausts it at 3000 m/sec (specific impulse 300 sec) with an impulse bit of 31.2 μ N-sec (7 μlb-sec). Langmuir probe measurements of electron density and temperature, a K-band microwave interferometer measure of density and collision frequency, spectroscopic analysis of ion species, and a Faraday cup measurement of ion velocity were all made. Ion velocities of approximately 40,000 m/sec indicate that the gas is only partially ionized. A thrust stand was constructed to measure impulse bit and specific impulse. The impulse bit is linear with capacitor energy (1.85 joules, normally). Modifications in the current return path to the capacitor which changes the magnetic field behind the exhaust were made. Specific impulse could be tripled, but impulse bit dropped by a like factor, with no improvement in efficiency.

Introduction

A PULSED plasma thruster (PPT) using an arc discharge across a Teflon surface (Fig. 1) has been successfully providing east-west stationkeeping on the Lincoln Laboratory Satellite, LES-6, for over a year now. The thruster has been described in detail in Ref. 1. With the success of this thruster, further development work was begun to improve the design. At the same time, a research and testing program was initiated to understand the physics of the thruster, to determine plasma and circuit parameters, to analyze the performance under configurational changes, and to do reliability and life tests. This paper reports the results of the program to date. Although the work is continuing and further understanding is required, a physical picture of the thruster operation is emerging, and a useful model which predicts the correct thrust and efficiency has been developed.

Understanding of the device was improved by determination of electron densities, temperature and collision frequency in parts of the exhaust with Langmuir probes and a K-band microwave interferometer, measurement of ion velocities with a downstream Faraday cup, estimation of conductivity from magnetic probes, and determination of ion species spectroscopically. Circuit parameters were measured or deduced from voltage and current waveforms, giving the magnetic pressure on the exhaust gas, and a thrust stand was built to measure impulse bit and specific impulse vs energy into the discharge.

From the aforementioned information, it was found that a fraction of the ablated Teflon is ionized and accelerated magnetically to approximately 40,000 m/sec, and the remaining neutral gas appears to be gas dynamically pushed off the Teflon face at a velocity approximately 3000 m/sec, the average exhaust velocity. The circuit model predicts an impulse bit of 32 μN-sec, agreeing with the thrust stand measurements. The model shows only 2.96% of the energy converted to thrust, with approximately 32% dissipated in the capacitor. The remaining energy is required to ionize and heat the plasma and to heat the electrodes of the discharge.

The Circuit Model

As shown in Fig. 1, a spring feeds the Teflon into the region where the charged capacitor plates are discharged across the Teflon face upon ignition of the spark plug. The discharge current is repelled by the return current to the capacitor through a back plate (the Teflon is fed through a hole in this back plate). This current repulsion, or magnetic pressure, accounts for the largest fraction of the thrust given to the exhaust gas. Figure 2a illustrates a simplified model in rectangular geometry, showing the current and magnetic field

Presented as Paper 70-179 at the AIAA 8th Aerospace Sciences Meeting, New York, January 19–21, 1970; submitted February 25, 1970; revision received August 19, 1970. This work was sponsored by the Department of the Air Force.

* Staff Member, Space Communications Division. Member AIAA.

† Associate Professor, Electrical Engineering Department.

‡ Associate Professor, Aeronautics and Astronautics Department. Member AIAA.

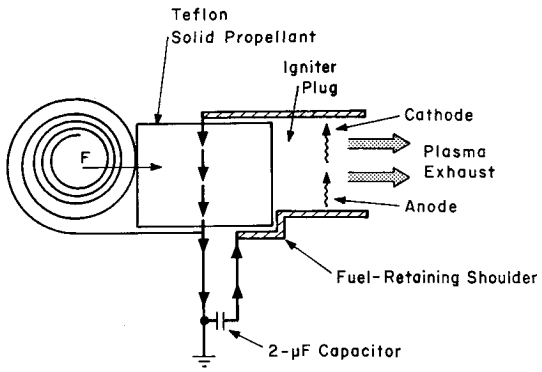

Fig. 1 Thruster schematic showing Teflon feed, discharge region and current path through the capacitor.

and a plasma sheet, which is assumed to move as a slug during the current "impulse." An equivalent RLC circuit[2] is shown in Fig. 2b. The capacitor has an internal resistance and inductance while the plasma has a time varying resistance. The inductance L_p comes from the flux between the plasma sheet and the back face.

The voltage at the terminals of the capacitor and a derived current waveform are shown in Fig. 3a. The differentiated terminal voltage is nearly I/C, except for small corrections from R_c and L. That is

$$-C(dV/dt) = I + R_cC(dI/dt) + LC(d^2I/dt^2) \qquad (1)$$

The inductance L is small, as can be seen by the current curve in Fig. 3a. At the instance of breakdown when the circuit is closed, the voltage $V_0 = 1360$ v divides between L and L_p. Since the current curve shows only a small drop at $t = 0$ from V_0, $L \ll L_p$. Now, given R_c and the initial values $I(0) = 0$, $I'(0) = V_0/(L + L_p)$, Eq. (1) can be integrated numerically to get the current curve. The resistance $R_c \approx 0.03\ \Omega$ and $L_p \approx 34\ nh$. The latter agrees with an approximate theoretical value $\mu_0 lh/w$. The effect of the capacitor inductance can be included when integrating[3] (and was in the current curve) by using an iterative method, as can the fact that L_p is varying as the sheet accelerates.

Given $I(t)$ and $L_p(t = 0)$ a determination can be made of the sheet position, plasma resistance, magnetic pressure (αI^2), and energy balance vs time. Figures 3b–d taken from Ref. 3 give these quantities. The total resistance is shown in Fig. 3b, of which a small fraction is the capacitor. During the first $\frac{1}{2}$ μsec, the circuit is overdamped ($R > R$ crit), which explains the "hitch" in the current waveform. In Fig. 3c the circuit dissipation (capacitor heating, electrode heating, ionization, plasma heating, and radiation) and $I^2(t)$ (proportional to magnetic pressure) are shown. Finally, Fig. 3d shows the division of energy with time.

The total impulse, integrating I^2, is 32×10^{-6} N-sec or 7 μlb-sec. Almost 32% of the energy is dissipated in the capacitor, while only 3% goes to kinetic energy. The measured mass ablation, 10^{-8} kg per shot, results in an average exhaust velocity of 3180 m/sec, which is a specific impulse of 312 sec. About 65% of the energy remains to be divided among electrode loss, ionization, heating, and radiation.

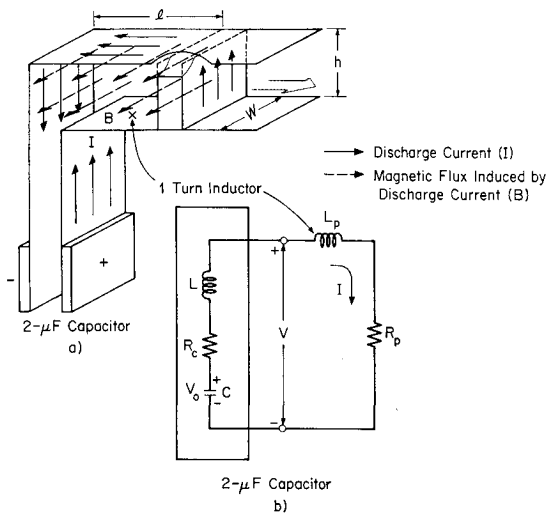

Fig. 2 a) Simple rectangular geometry model showing the current path, magnetic flux and the plasma slug; b) circuit representation of the model; $L \equiv$ capacitor inductance ($L \ll L_p$), $R_c \equiv$ capacitor resistance, $C \equiv 2\ \mu f$ $L_p \equiv$ time-varying inductance due to flux behind plasma slug, and $R_p \equiv$ time-varying plasma resistance.

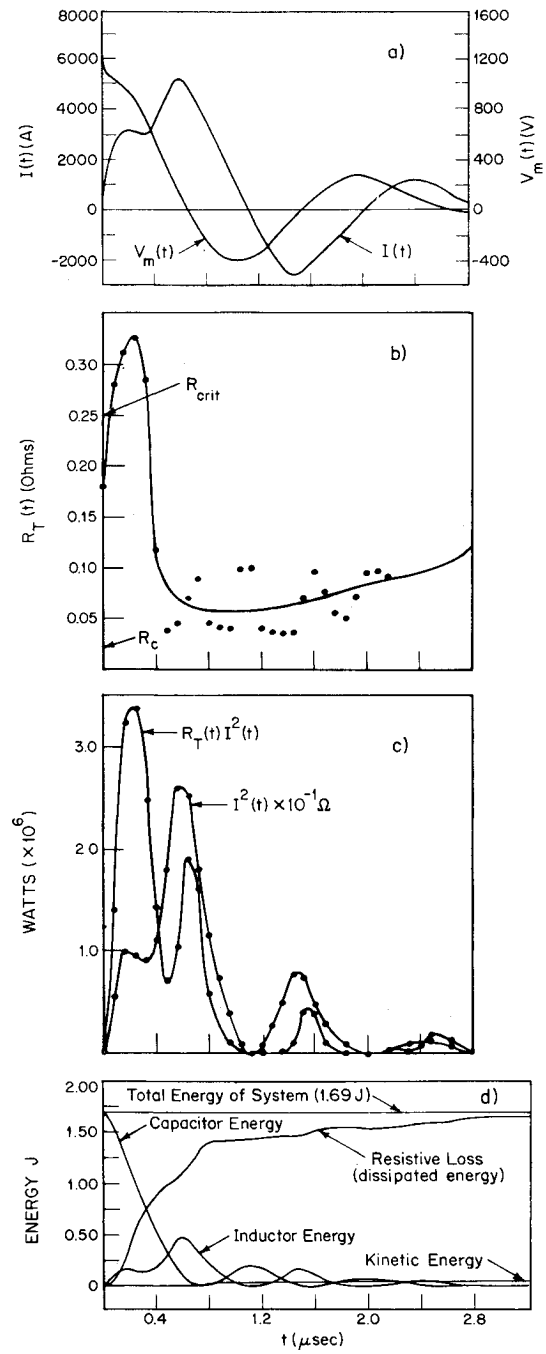

Fig. 3 a) Measured voltage waveform [$V_m(t)$] at capacitor terminals and deduced current waveform [$I(t)$]; b) total circuit resistance; c) magnetic pressure [proportional to $I^2(t)$], total power loss; and d) division of total energy calculated from a).

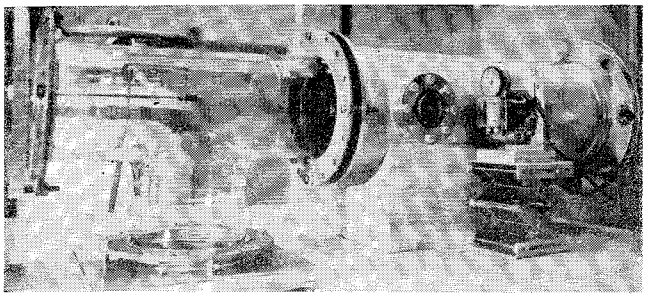

Fig. 4 Experimental chamber and diagnostic access ports.

Momentum Relations

A momentum balance may be written with the Maxwell stress tensor T_{ij}, whose divergence gives the particle electromagnetic force density $\rho E_j + (\mathbf{J} \times \mathbf{B})_j$, and the particle stress tensor $P_{ij} = nm\langle v_i v_j \rangle$, whose divergence gives the gas dynamic force density. For an isotropic velocity distribution, that force is simply a pressure gradient, with nkT the particle pressure. The momentum equation relates these tensors to the particle and photon momentum densities $p_j = nm\langle v_j \rangle$ and $g_j = (\mathbf{E} \times \mathbf{H})_j/c^2$. If the entire exhaust gas is surrounded by surface $\bar{S}$, enclosing volume V, the relation is[4]

$$\iiint \nabla \cdot \bar{\bar{T}} + \bar{\bar{P}})dV + (\partial/\partial t)\iiint(\bar{p} + \bar{g})dV = 0 \quad (2)$$

In words, the rate of change of momentum is balanced by the forces (divergence of stress). The balance in the last section neglected $\bar{\bar{P}}$ and $\bar{g}$.

The first integral in Eq. (2) can be converted to a surface integral, hence the momentum given to the gas (and photons) can be found by evaluating only the surface stress. The stress is assumed nonzero only over the Teflon for the component of Eq. (2) in the direction of the exhaust. Further, if the magnetic field there is parallel to the surface and constant, and if the velocity distribution is isotropic

$$\left(\frac{1}{2}\mu_0 H^2 + nkT\right)A = \frac{\partial}{\partial t}\iiint\left[nm\langle v_z\rangle + \frac{(\mathbf{E} \times \mathbf{H})_z}{c^2}\right]dV \quad (3)$$

where A is the area of the exposed surface. It can now be argued that the photon momentum E_f/c (E_f is the photon energy) is small compared to the particle momentum (E_p/v_e) owing to the great disparity in velocities ($v_e \ll c$).

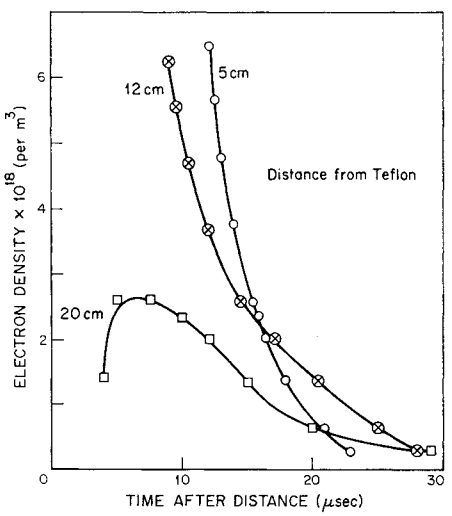

Fig. 5 Microwave interferometer measurements of density with time after the discharge for several positions downstream.

Integrating Eq. (3) to infinite time and approximating H by I/w

$$\int_0^\infty \left(\frac{1}{2}\frac{\mu I^2}{w^2} + nkT\right) hwdt = Nm\langle v_z\rangle \quad (4)$$

where Nm is the total exhaust mass (10^{-8} kg). This relationship was used in the previous section, except that nkT was neglected.

Each species in the exhaust (electrons, ions, and neutrals) obey a similar equation, except for terms describing forces between species by collisions (of course, there is no electromagnetic force on the neutrals). If the only interest is in the motion of the entire exhaust, Eq. (4) will give correct results even with neutral particles in the exhaust, because momentum gained by charged particles through magnetic pressure forces can be transferred to neutrals but not lost.

To estimate gas dynamic forces it is necessary to know the density and temperature of each species. Later on it will be shown that there may be a small contribution to the electron momentum by electron neutral pressure. Neither of these appear at this time to be of the same order as the momentum transferred via magnetic pressure.

Plasma Diagnostics

A stainless steel vacuum chamber, shown in Fig. 4, with two ports for viewing the discharge or inserting diagnostics, was constructed. The thruster can be slid about 18 in. along a track of the chamber. The chamber is mounted on a glass tee to provide a pumping port. A Faraday cup or various probes can be inserted at one end of the tee and moved axially into the throat of the thruster.

A K-band microwave interferometer with horns inserted inside the two ports was used to determine electron density vs distance and time. The cutoff density is $7 \times 10^{12}/\text{cm}^3$, and is exceeded during a large time interval near the throat. Figure 5 shows the density $n(x,t)$ as a function of time. It was found, by plotting the initial cut off time vs distance, that the plasma exhaust velocity is near 35,000 m/sec. This was confirmed by Faraday cup data to be discussed shortly.

The electron temperature can in principle be measured with a Langmuir probe, sampling the signal for a 1 μ-sec interval at times of interest. From the sampled currents vs probe voltage, a reasonable probe characteristic can be constructed during the afterglow, at least for times greater than 4μsec follow-

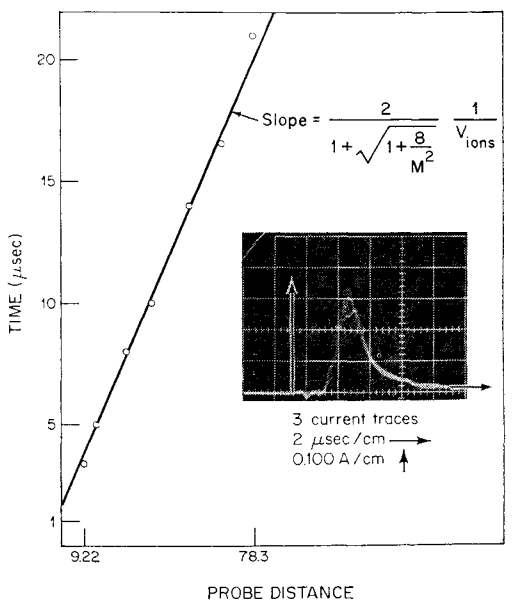

Fig. 6 Peak current arrival time at a Faraday cup vs distance and a typical collected current trace (inset).

ing capacitor breakdown. Large floating potentials (several hundreds of volts) during breakdown make measurements difficult at that time. Even in the afterglow measurements are uncertain; nonetheless those probe measurements give temperatures ranging from 20 to 25 ev. An attempt to verify this temperature by measuring relative intensities of C_{IV} to C_{III} and C_{III} to C_{II}[5] gave temperatures in the range of 3–8 ev. The uncertainy comes from lack of knowledge of electron density that is required for this method. Given the methods employed in measuring temperatures, the results are not as accurate as we would like. However, temperatures in this range are not surprising for a low-pressure arc discharge. In fact, spectral lines of C_{IV} and F_{IV} were seen, which tends to support an elevated temperature.

Magnetic probes along the thrust axis can be used to determine the diffusion of the current (or magnetic field) into the plasma, provided the magnetic Reynolds number is low. The surface current waveform simply propagates into the conducting medium, and from the skin depth an estimate of conductivity can be made. This estimate gives $\sigma \approx 10^4$ mho/m, from which is determined a magnetic Reynolds number of order unity. Thus, the field lines are neither frozen into the moving plasma, as assumed in the circuit model, nor do they simply diffuse into the exhaust region.

One of the more useful diagnostic measurements is the Faraday cup signal at various downstream positions. A 1-mm diam hole in the front face of the cylindrical chamber surrounds a negatively biased collecting electrode, and the collected ion current is displayed on an oscilloscope. To understand how the waveform varies with distance between nozzle and cup, it is assumed the velocity is a drifting Maxwellian. The initial distribution is a delta function (point source) at the Teflon face, the origin of the coordinate system.

For later times the distribution is determined from the free streaming solution to the Boltzmann equation, so the distribution function is

$$f(\mathbf{r},\mathbf{v},t) = n\left(\frac{m}{2\pi kT}\right)^{3/2}\delta(x - v_x t)\delta(y - v_y t)\delta(z - v_z t) \times \exp\{-(m/2kT)[(v_x - v_0)^2 + v_y^2 + v_z^2]\} \quad (5)$$

where n is the density and v_0 the drift velocity along the x axis (the exhaust direction). Integrating $v_x f(\mathbf{r},\mathbf{v},t)$ gives the current for a Z-times ionized atom, through a hole with radius ρ

$$I(t) = \frac{ZenM^3 t_0^3 \rho^2}{(\pi^{1/2} L^2 t^4)} e^{-M^2(t_0/t-1)^2} \quad (6)$$

where $M_s = mv_0^2/2kT$ is an artificial "Mach number," L is the distance to the cup, and $t_0 = L/v_0$ is the time of flight. This expression has a maximum near t_0, namely at $t = 2t_0/91 + (1 + 8/M^2)^{1/2}$. For $M \gg 1$ the peak is at $t = t_0$ and the slope of t_0 vs L gives the ion velocity v_0. In Fig. 6, that data is displayed which gives an ion velocity $v_0 = 40{,}000$ m/sec for large M. Estimates of M can be made from the spreading of the waveform. We find $M \sim 3.5$, corresponding to $T_i = 35$ ev. This value would appear to be too high, and the error comes from assuming the current to the Faraday cup is from singly ionized species having the same velocity. More recent measurements show that there are doubly and triply ionized species all with different velocities.[6] Hence the spread is not a true ionized spread. The actual ion temperature will therefore be lower, but we have no measurements to date.

The peak value of $I(t)$ is $I(t_0)$ (for $M \gg 1$), which is seen to be inversely proportional to L^3. In Fig. 7, a log$I$ vs log$L$ plot displays this dependence, lending credence to the theory.

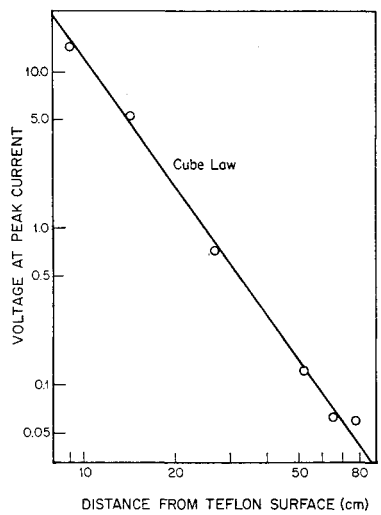

Fig. 7 Peak current amplitude vs distance showing (dist)$^{-3}$ dependence.

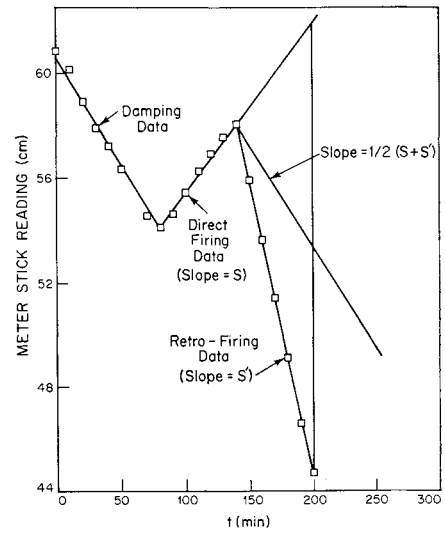

Fig. 8 Amplitude of pendulum thrust stand arm vs time during free decay, direct firing, and retrograde firing.

Thrust Measurements

Thrust measurements were made on a pendulum type stand constructed at M.I.T.[7] The system was mounted in a bell jar at pressures below 2×10^{-6} mm. Damping times of approximately 13 hr were achieved for deflections less than 5°. The amplitude was monitored optically using a laser and a mirror mounted on the arm. Thrust is determined by monitoring the damping rate for about an hour, then firing the thruster at the bottom of each swing for another hour, and finally retrofiring the thruster at the bottom of each swing. The amplitude vs time on such a sequence is shown in Fig. 8,

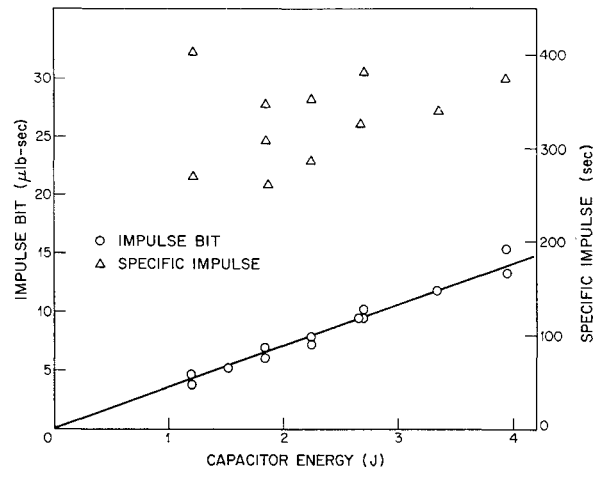

Fig. 9 Specific impulse and impulse bit vs stored capacitor energy.

giving thrust data accurate to approximately 5%. By weighing the fuel after the run, the mass consumption (specific impulse) is then found.

Attempts were made to change the performance of the thruster by altering the current return path to the capacitor. With current loops on each side of the exhaust channel, oriented so as to increase or decrease the flux behind the discharge current sheet [see Fig. 2a], the specific impulse I_{sp} and and impulse I_p were measured. In general, I_{sp} could be increased, but I_p always decreased when it did. Efficiencies remained nearly the same, but I_{sp} could be tripled.

Measurement of I_p and I_{sp} in the normal configuration were made for a range of capacitor energies E_c. Figure 9 shows that I_p vs E_c is linear while I_{sp} vs E_c did not follow a predictable pattern. Fuel consumption is probably sensitive to the Teflon condition and nozzle contamination, thereby explaining the latter results. Peak current in the circuit was found to be proportional to the capacitor voltage for $500 \leq v_c \leq 2000$ volts, also predicting a linear I_p vs E_c relationship if magnetic pressure provides the thrust.

Summary of Results

A simple slug model of the thruster has been used to explain many of the salient features of the device. A 5000 amp current pulse ablates 10^{-8} kg of Teflon (6×10^{16} molecules of C_2F_4) and ionizes some fraction of it. Nearly 70% of the energy is expended in ionizing plasma heating electrons (the bulk of that 70%), heating the electrodes, and ablating and dissociating molecules. The latter energy is approximately 4%. About 30% is lost in the capacitor.

Magnetic pressure on the slug can account for the total momentum given to the gas. This computation gives 3000 m/sec, which agrees with thrust stand measurements and since ion velocities are approximately 40,000 m/sec, it is apparent that only part of the gas is ionized. These data could be explained assuming $\frac{3}{40}$ of the gas is ionized and accelerated during the current pulse, the remaining neutrals oozing off the hot Teflon following that. The ions then freestream away without any neutral collisions, while the neutrals that follow have negligible velocity because the neutral pressure is small. It is also possible that all the gas is ablated during the current pulse, but is only partially ionized.

Further experiments on neutral velocities are needed, as are density measurements in the arc; only then can a determination be made of the processes that take place at the surface. If the gas pressure at the Teflon were known, further insight into the process would be gained.

Estimates of partial pressures can be made. There are 3.6×10^{17} neutrals, so if they occupy 1 cm^3 during the pulse and it is assumed they are at 10,000°K (1 ev), their pressure is approximately $6 \times 10^4\ N/m^3$. The peak magnetic pressure $\frac{1}{2}\mu_0 (I/w)^2$ is approximately $16 \times 10^4\ N/m^3$. The ion pressure is probably smaller than the neutral pressure because the temperatures are probably comparable, whereas the ion density is much less. Electron pressure could be significant if the 20 ev figure is correct, but if there were 20 neutrals/electron, the electron pressure would just equal the neutral pressure. Further measurements are again needed.

Attempts to improve thruster performance by altering the return path gave mixed results. No increase in efficiency was seen, but I_{sp} could be increased at the expense of thrust. Measurements showed thrust to be proportional to energy stored in the capacitor and indicated that efficiency also increased with increasing energy.

From the results to date, some understanding of the thruster has emerged. Some of the quantitative information missing now will help in understanding discharge, ablation, ionization, and thrust phenomena.

References

[1] Guman, W. J. and Nathanson, D. M., "Pulsed Plasma Microthruster Propulsion System," *Journal of Spacecraft and Rockets*, Vol. 7, No. 4, April 1970, pp. 409–415.

[2] Jahn, R. G., *Physics of Electric Propulsion*, McGraw-Hill, New York, 1968, Chap. 9.

[3] Waltz, P., "Analysis of a Pulsed Electromagnetic Plasma Thruster," M.S. thesis, 1969, Electrical Engineering Dept., M.I.T., Cambridge, Mass.

[4] Schmidt, G., *Physics of High Temperature Plasma*, Academic Press, New York, 1966, p. 65.

[5] Griem, H. R., *Plasma Spectroscopy*, McGraw-Hill, New York, 1964, pp. 275–276.

[6] Guman, W. J., Vondra, R. J., and Thomassen, K., "Pulsed Plasma Propulsion System Studies," AIAA Paper 70-1148, Stanford, Calif., 1970.

[7] Radley, R. J., Jr., "Study of a Pulsed Solid Fuel Microthruster," M.S. thesis, 1969, Dept. of Aeronautics and Astronautics, M.I.T., Cambridge, Mass.